Title: The effect of metal (Nb, Ru, Pd, Pt) supported on SBA-16 on the hydrodeoxygenation reaction of phenol

Authors: Agnieszka Feliczak-Guzik, Paulina Szczyglewska, Izabela Nowak

PII: S0920-5861(18)30857-5
DOI: https://doi.org/10.1016/j.cattod.2018.06.046
Reference: CATTOD 11535

To appear in: *Catalysis Today*

Received date: 29-3-2018
Revised date: 18-6-2018
Accepted date: 30-6-2018

Please cite this article as: Feliczak-Guzik A, Szczyglewska P, Nowak I, The effect of metal (Nb, Ru, Pd, Pt) supported on SBA-16 on the hydrodeoxygenation reaction of phenol, *Catalysis Today* (2018), https://doi.org/10.1016/j.cattod.2018.06.046

The effect of metal (Nb, Ru, Pd, Pt) supported on SBA-16 on the hydrodeoxygenation reaction of phenol

Authors

Agnieszka Feliczak-Guzik, Paulina Szczyglewska, Izabela Nowak

Adam Mickiewicz University in Poznan, Faculty of Chemistry, 89b Umultowska, 61-614

Poznan, Poland;

Graphical abstract

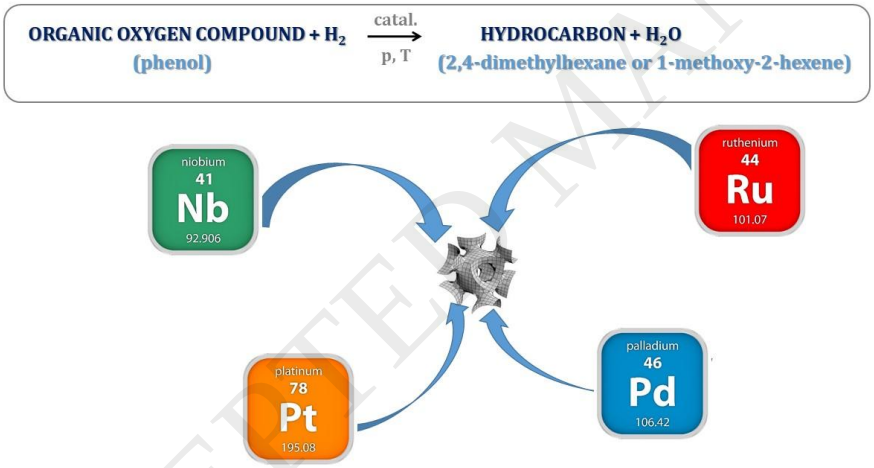

Highlights

- Variation of impregnation process on physicochemical properties of the systems obtained
- Application of mesoporous materials with Nb, Ru, Pt, Pd in the catalytic reactions
- Effect of type of active phase (metal) on HDO reaction

Abstract

Ordered silica materials of SBA-16 type were synthesized, characterized as to their physicochemical properties and used as supports of the active phases which were niobium, ruthenium, palladium or platinum ions. Physicochemical properties of the systems obtained were determined by XRD, N_2 sorption and TEM methods. Then the materials were used as catalytic systems in the process of phenol hydrodeoxygenation. The reaction was carried out in the range 90-130°Cunder hydrogen pressure of 2,5-6 MPa. The effects of three variables on the course of the process were evaluated:(i) temperature, (ii) hydrogen pressure, (iii) type of active phase (metal). The main product of the reaction with the use of catalysts SBA-16/Ru, SBA-16/Pd, SBA-16/Pt was 2,4-dimethylhexane, while when using SBA-16/Nb, the main product was 1-methoxy-2-hexene. In the reaction conditions applied, 100% of phenol conversion was achieved. Direct effect of the reaction conditions, i.e., temperature and hydrogen pressure on the course of the process was observed.

Keywords

Hydrodeoxygenation, phenol, niobium, ruthenium, palladium, platinum, SBA-16

Introduction

Increasing demand for energy and gradual depletion of fossil fuels have stimulated the search for alternative energy sources [1, 2]. Because of the rich composition, common occurrence and renewability, lignocellulose biomass is a valuable raw material for production of

biofuels and different chemical substances [3-6]. From among many technologies for biomass conversion, fast pyrolysis is one of the best as it permits reaching conversions of the initial biomaterials of up to 70 wt.% into a dense liquid known as biooil [7,8]. The liquid fuel obtained as a result of biomass pyrolysis is a promising semiproduct that can be an alternative to fossil fuels. However, because its low quality caused by the high content of water (up to 30 wt.%) and the content of reactive chemical compounds such as phenols, carboxylic acids, aldehydes and ketones, whose total content reaches even up to 50 wt.%, direct use of biooil as a biofuel is impossible [9, 10]. Its quality must be improved so that it would be characterized by higher calorific values, higher thermal and chemical resistance. Such an improvement requires first of all a reduction of the content of oxygen atoms in the system as their presence is the main obstacle in using the pyrolytic oil as a substitute of fossil fuels [11, 12].

Catalytic hydrodeoxygenation (HDO) is one of the most effective methods for biooil improvement. This process is performed at high temperatures (150-450°C)under high hydrogen pressure (5-25MPa) in the presence of different catalysts [13, 14]. Finally, this technology permits a conversion of organic aromatic compounds, present in biooil and containing in their structure oxygen atoms, into chemical compounds of higher H/C ratio at a lower O/C ratio, which can even lead to obtaining hydrocarbons [15-17]. In laboratory scale hydrodeoxygenation is performed using the model chemical compounds, identical to those present in biooil. The functional groups most often occurring in biooil as methoxyl groups (-OCH_3) and hydroxyl groups (-OH), so the model compounds usually used in investigation are anisole, phenol, guaiacol or catechol [18, 19]. High yield of the process depends to a great degree on the choice of the catalytic system, the most effective ones employ transition metal atoms (Nb, Ru, Pd, Pt), which easily activate hydrogen and ensure getting desired reaction products [20, 21]. The metals

are deposited on supports whose role is to ensure the best possible dispersion of the active phase and improvement of the thermal and mechanical strength of the system [22, 23]. These criteria are met by ordered mesoporous silica materials, which thanks to their unique morphology, i.e. well-developed surface area and uniform pore system, are perfect supports for transition metals [24-26]. The silicas of the types MCM (Mobil Crystalline Material), KIT (Korean Institute of Technology) or SBA (Santa Barbara Amorphous) with transition metal ions on the surface have been successfully applied in a number of catalytic processes involving gas hydrogen [24, 27-31].

This paper presents results obtained for hydrodeoxygenation of phenol. This process was performed in relatively mild conditions: T=90-130°C and pressure pH_2=2,5-6 MPa, applied to minimize the use of energy. The catalysts were heterogeneous systems of metallic niobium, ruthenium, palladium or platinum as the active component supported on mesoporous silica of SBA-16 type. The study was aimed checking the effects of (i) temperature, (ii) pressure and (iii) type of metal used on the degree of phenol conversion and forming reaction products.

Experimental

Catalyst preparation

The unmodified mesoporous silicas of SBA-16 type were synthesized by the standard sol-gel method. Laboratory vessels were charged with 4.8 g of triblock copolymer of ethylene oxide and propylene oxide, Pluronic F127 (Sigma-Aldrich), to which 460.6 g of distilled water and 192 g 2M of hydrochloric acid (Chempur) were added. After dissolution of the structure-directing agent (i.e. Pluronic F127), 20.2 g of TEOS (Sigma-Aldrich) were added dropwise. The contents were stirred on a magnetic stirrer for 0.5 h at room temperature. Then the system with the precipitate was aged in a laboratory drier for 48 h at 90°C. The precipitate obtained after ageing was filtered off on a funnel, washed with distilled water and dried in air at room

temperature. The materials were subjected to calcination in order to remove surfactants from silica pores (6 h, 550°C). Then the unmodified SBA-16 type silica was subjected to incipient wetness impregnation. The vessel with a weighted portion of the support was dropwise charged with a water solution of $(NH_4)_3NbO(C_2O_4)_3(H_2O)$ (Sigma Aldrich), ethanol solution of $RuCl_3*H_2O$ (Alfa Aesar), ethanol solution of $PdCl_2$ (Alfa Aesar) or ethanol solution of $H_2PtCl_6*6H_2O$ (Alfa Aesar). The mass fraction of metals was always kept as 3 wt.%. in respect to the support. The vessel with the impregnated support was tightly closed with polyolefin-paraffin foil and left to rest for 24 h. Then the catalysts were dried for 1 h at 30°C, for 1 h at 40°C and 18 h at 60°C. Next, they were reduced in a tube furnace in hydrogen atmosphere in order to obtain monometallic metal species on a mesoporous support. At first in order to remove air from the system argon of 5.0 purity (N5.0; Linde Gas Poland) (50 cm^3/min) was blown through the system at room temperature for 0.5 h, then hydrogen was blown (50 cm^3/min) and after 0.5 h the heating was started. Depending on the metal used, the catalysts were reduced for 3 h at 400°C (niobium), 250°C (ruthenium), 350°C (palladium), 250°C (platinum).

Catalyst characterization

Physicochemical properties of all catalysts were determined on the basis of X-ray diffraction (XRD), transmission electron microscopy (TEM) and low-temperature adsorption/desorption of nitrogen. XRD study was performed on a Bruker AXS D8 Advance diffractometer with a Johannson monochromator. The source of CuK_αradiation generated radiation of the wavelength α=0.154 nm in the 2Θ range 0.6 - 10° with the accuracy to 0.02° (small-angle range) and in the 2Θ range 4 - 60° with the accuracy to 0.05° (wide-angle range).TEM images were recorded on a JEOL JEM 1200 EX II microscope using the electron beam of 80 kV.The low-temperature nitrogen adsorption/desorption were carried out using Nova

1200e Quantachrome at 176°C, after preliminary degassing of the sample in vacuum at 350°C for 24 h. The specific surface area of the catalyst was determined by BET (Brauner-Emmet-Teller) method, while the pore volume was found by the modified BJH (Barret-Joyner-Halenda) method proposed by Kruk, Jaroniec and Sayari (KJS-BJH). Moreover, all materials were characterized by thermogravimetry (TG), X-ray photoelectron spectroscopy (XPS), SEM/EDX (scanning electron microscopy with EDX) and temperature programmed reduction (H_2-TPR) – see supporting information.

Experiments (HDO of phenol)

Phenol hydrodeoxygenation was carried out in a high-pressure reactor (CAT 24 HEL) placed on a magnetic stirrer. Prior to the proper reaction, all catalysts were activated in a muffle furnace at 400°C for 4 h. Then, the appropriate catalysts in the amounts of 0.005 g were placed in glass reaction vessels, to which 0.05 g of phenol (Sigma-Aldrich) were added and the contents were flooded with 1 g of dodecane (Sigma-Aldrich) used as a solvent. The glass vessels were equipped with magnetic stirrers. The reaction mixtures were placed in a high-pressure reactor that was tightly closed and three times washed with argon N5.0 in order to remove air from inside the reactor. Then the reactor was twice washed with hydrogen N5.0 and finally it was filled with hydrogen to a pressure of 2.5, 4 or 6 MPa. Then a desired temperature of 90, 110or 130°C was set and stirring was started (700 rotation per minute). The reaction was performed for 4 h and then the reactor was cooled and gas was released.

Product analysis

After removal from the high-pressure reactor, the reaction mixtures were subjected to stirring in order to separate the liquid reaction products from the catalyst, and the products were subjected to chromatographic analysis on a gas chromatograph with a flame-ionization detector

(VARIAN 3900 GC; a capillary column CPWAX57CB:length 25 m, diameter 0.32 mm, film thickness 1.2 μm) and a gas chromatograph with mass detector (VARIAN 4000 GC; acapillary column CPWAX57CB: length 25 m, diameter 0.32 mm, film thickness 1.2 μm). The reaction products were identified by two methods, on the basis of retention times of chemical compounds compared with retention times of available standards and using the compounds library NIST.

Results and discussion

X-ray diffraction analysis

XRD measurements in the small-angle range provide information on the degree of ordering of the obtained materials structure (Figure 1 left). XRD diffractograms of all samples show one intensive reflection at 2Θ=0.9° whose presence is the evidence of their ordered structures. SBA-16 type silica has cage-like cubic structure of space group Im3m.

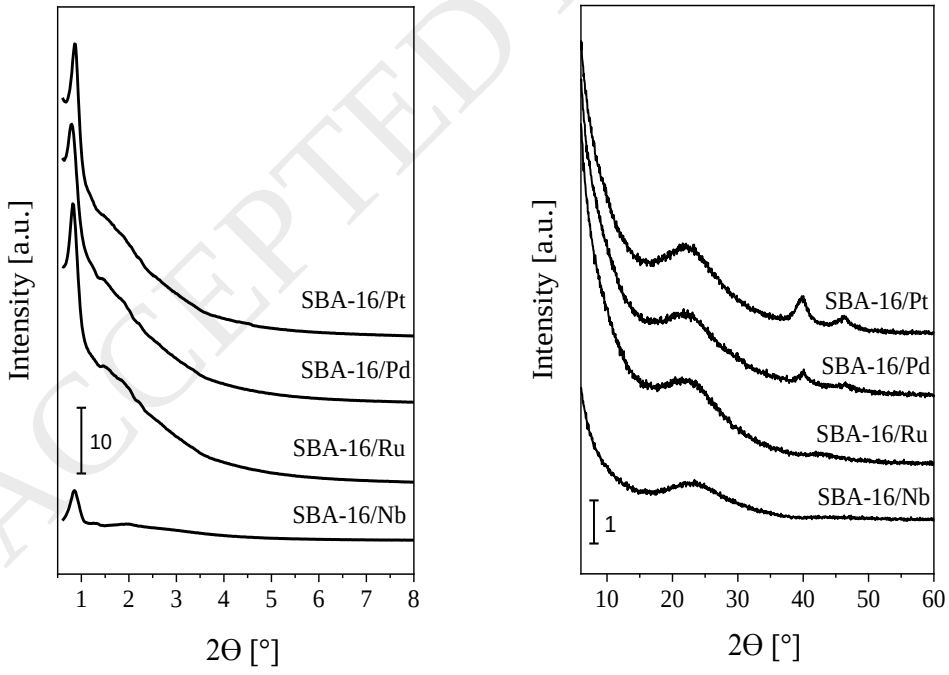

Figure 1.Small- (left) and wide-angle (right) XRD patterns of SBA-16 mesoporous silica containing different metal atoms.

XRD diffractograms in the wide-angle range provide information confirming the presence of relevant metals introduced by incipient wetness impregnation (Figure 1 right). Only for two from among all samples studied: SBA-16/Pd and SBA-16/Pt, the reflections from metallic species of relevant metals were observed. The diffractogram of sample SBA-16/Pd shows two reflections at 2Θ=40.2° and 2Θ=46.7°. For sample SBA-16/Pt also two reflections appear at 2Θ=39.8° and 2Θ=46.3°. The presence of these reflections confirms the successful introduction of Pd and Pt atoms into the silica matrix, which is additionally confirmed by TEM images. The diffractograms of SBA-16/Nb and SBA-16/Ru do not show the reflections testifying to the presence of the respective metal ions in the silica structure, however, it is not equivalent to the absence of these metals. The lack of reflections may be a consequence of too small sizes of the crystallites introduced. The presence of Nb and Ru onto the SBA-16 type silica is confirmed by TEM images.

Low-temperature N_2 adsorption/desorption measurements

The low-temperature nitrogen adsorption/desorption is used for characterization of porous materials. On the basis of the isotherms obtained it is possible to determine the surface area, pore volume, pore diameter and pore size distribution. Figure 2 presents the low-temperature nitrogen adsorption/desorption isotherms for all samples obtained. The shape of isotherms is characteristic of all mesoporous materials and is labelled as IVa according to IUPAC classification [32, 33]. The isotherms showed one hysteresis loop. For the samples SBA-

16/Ru, SBA-16/Pd and SBA-16/Pt the hysteresis loop was of similar size, which indicated similar total pore volume, and appeared in the relative pressure range p/p_0=0.45-0.7.

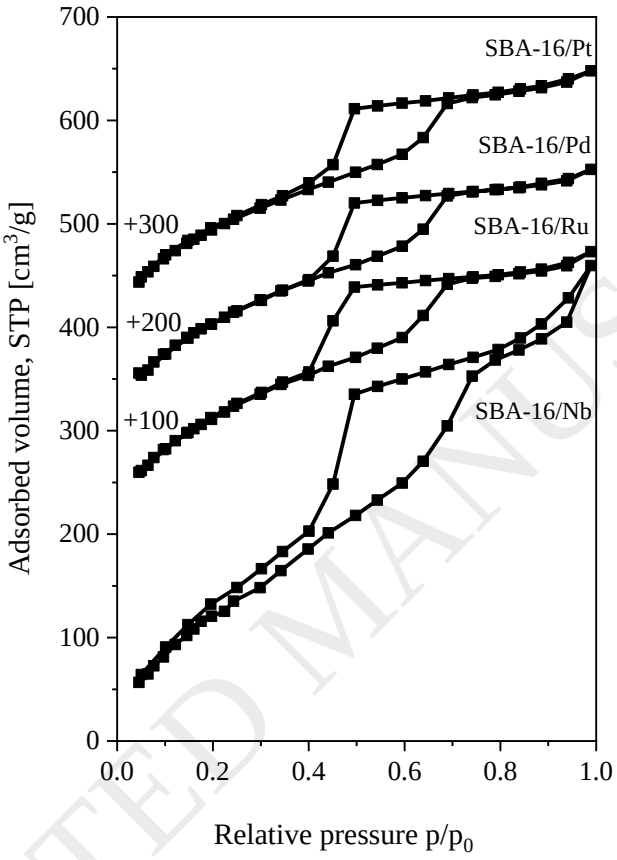

Figure 2.Isotherms of the SBA-16 mesoporous silica containing different metal atoms.

Table 1 presents the textural parameters of the materials studied. All silicas are characterized by relatively large surface areas (BET). The largest surface area of 920 m^2/g was found for SBA-16/Nb, while the smallest for SBA-16/Pt (704 m^2/g). The other textural parameters of the silica samples that is pore volume of over 0.5 cm^3/gand average pore size varied from6.3 to 7.4 nm, were very similar. The generally similar textural parameters of all

silicas mean that incipient wetness impregnation had practically no effect on the quality of the silicas (structure and textural properties).

Table 1. Structure and textural properties of all catalysts.

Catalysts	Surface area (BET) [m^2/g]	Total pore volume [cm^3/g]	Pore size (BJH ads.) [nm]
SBA-16/Nb	920	0.6	7.4
SBA-16/Ru	769	0.6	6.3
SBA-16/Pd	743	0.5	6.4
SBA-16/Pt	704	0.5	6.3

TEM images

The TEM images provided the information on the degree of structural ordering and the presence of transition metals in the samples. As follows from the TEM images presented in Table 2, all synthesized samples show high structural ordering, which has been also indicated by XRD results. The dark points visible in the TEM images are the evidence of transition metal presence in the samples, which confirms the effectiveness of incipient wetness impregnation method. The introduced transition metals show good dispersion and their clusters have similar sizes within a given sample.

Table 2. TEM images of the SBA-16 silica containing various transition metal atoms (a-Pt, b-Pd, c-Ru, d-Nb).

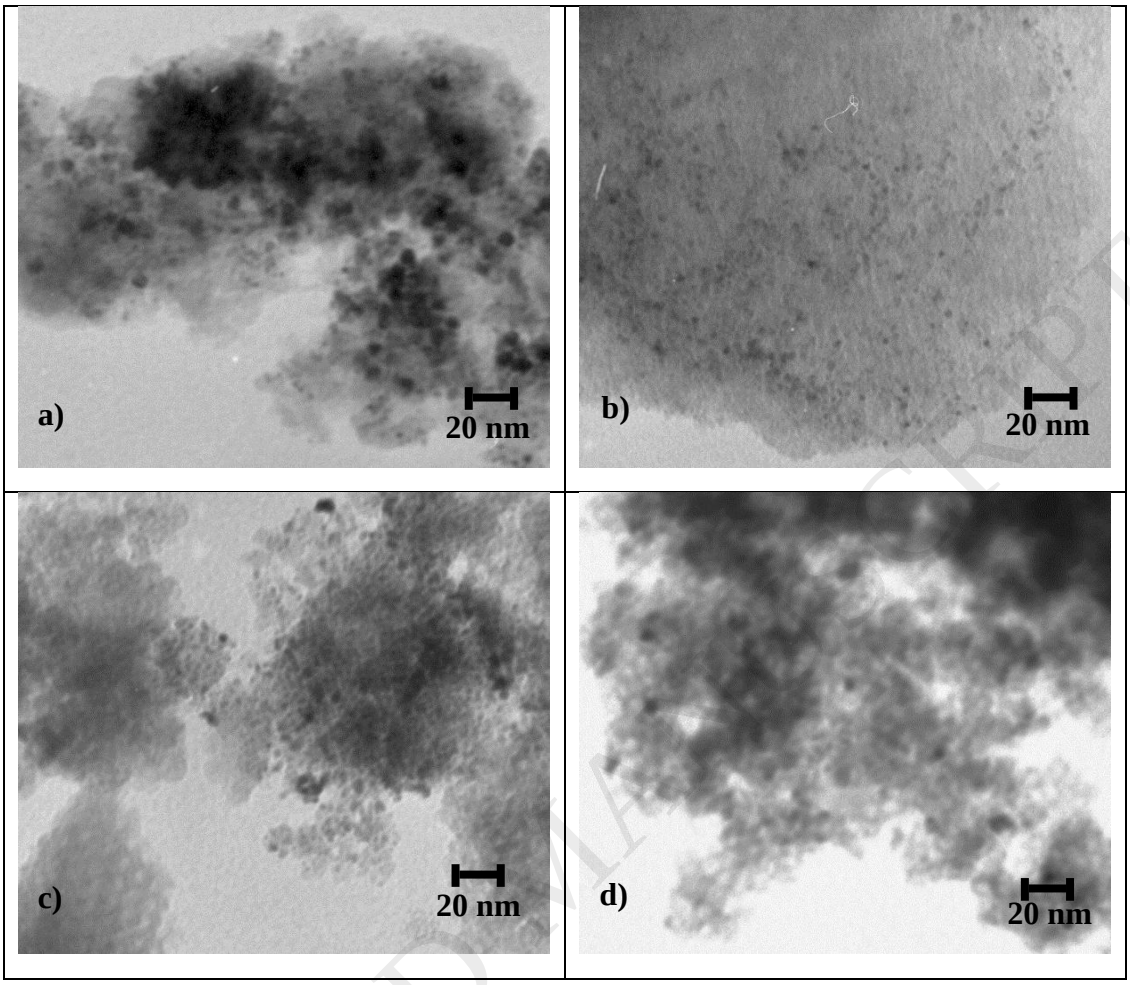

The results of the SEM-EDX analysis show homogeneous distribution of the introduced metal. The metal content was presented in Table S1 (see Figure S1 and Table S1 in supporting information). Thermal stability of the samples were described in supporting information. All the materials are stable at the temperature applied for HDO.

The results of phenol HDO reaction

It is known from literature that phenol molecules under elevated pressure and temperatures (the conditions typical of hydrodeoxygenation) undergo different transformations, e.g. hydrogenation, dehydration, demethoxylation, demethylation and methylation [34, 35].The type of reaction

products depends not only on the reaction conditions but also on the type of catalyst used. By chromatographic methods the following products of HDO of phenol: cyclohexene, 1-methoxycyclohexene, cyclohexanol, 1-methoxy-2-hexene and 2,4-dimethylhexane were identified. The products labelled as "other" are the undesirable products of phenol addition, mainly naphthalene derivatives. Figure 4 presents a scheme illustrating the possible transformations of phenol molecules in the process performed. On the basis of the identified products of HDO reaction of phenol, we proposed two pathways of transformations (Fig. 4). According to the first pathway, at first the aromatic ring is hydrogenated, which leads to cyclohexanol formation, then cyclohexanol is dehydrated to cyclohexene. The second pathway leads to 1-methoxycyclohexene as a result of partial hydrogenation of the aromatic ring and attachment of a methyl group to the oxygen atom. Then, the C-C is broken, the cyclic character is lost and 1-methoxy-2-hexene is produced. Finally, after demethoxylation and attachment of two methyl groups, 2,4-dimethylhexane is obtained. It is important to stress that such mechanism can be observed only in the case of Brønsted acid sites. It has been largely recognized that the transmethylation reaction is induced by a proton that dissociates from the acid site and launches an electrophilic attack on the reactant [34]. The domination of this pathway may be related to the character of transition metal and acidity of the support used as the energy needed for hydrogenation of aromatic ring is lower than that needed to break the bond between the carbon atom from the aromatic ring.

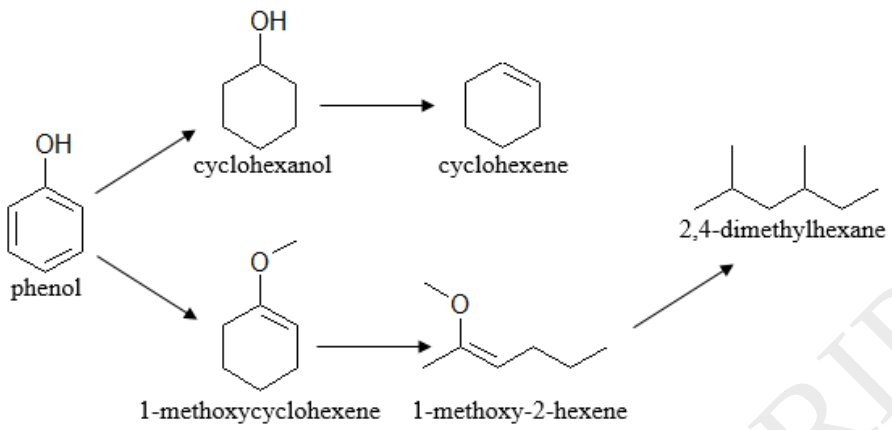

Figure 4. Scheme of the possible routes of phenol hydrodeoxygenation.

It is interesting to note that kinetic profiling revealed ring hydrogenation as the dominant pathway during the first hour of reaction. Afterwards, slower C=C hydrogenation versus C=O hydrogenation occurs. Further kinetic studies are currently underway to elucidate the rate-determining step in phenol HDO, in addition to the impact of metal loading, and the selection of phenolic substrate (e.g. guaiacol), in order to optimize the yield of products and establish the generic applicability of supported SBA-16 in biooil HDO.

Figures 5-8 illustrate the phenol conversion depending on the catalyst and reaction conditions applied. Tables 3-6 present the reaction products and selectivities of their formation.

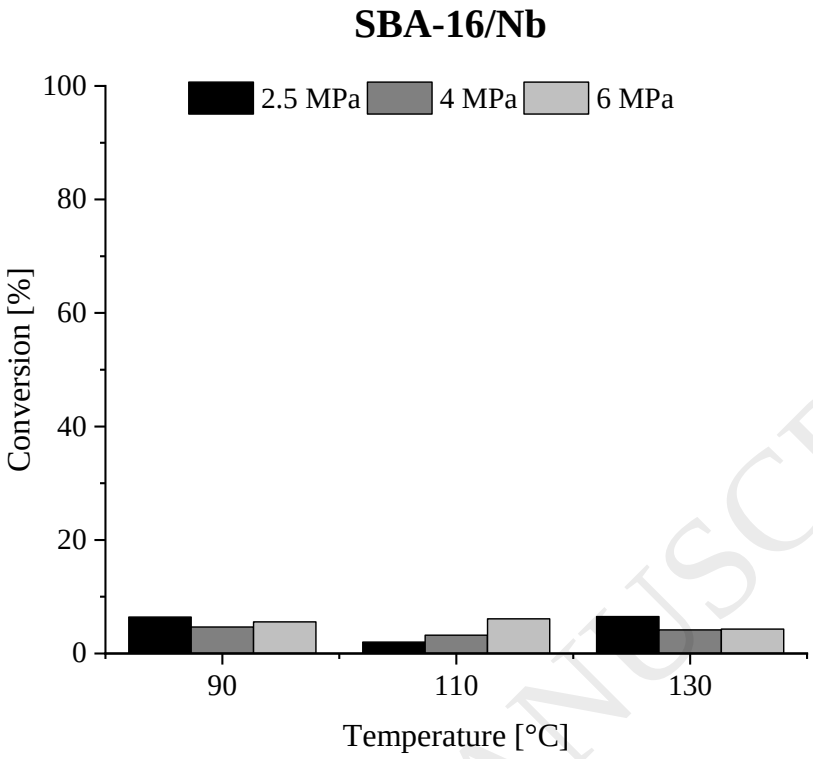

Figure 5. Conversion of phenol over SBA-16/Nb catalyst under different conditions.

Table 3. Product distribution for phenol HDO over SBA-16/Nb catalyst under different conditions.

Catalyst	Temperature [°C]	Pressure [MPa]	Selectivity [%]					
			cyclohexene	1-methoxycyclohexene	cyclohexanol	1-methoxy-2-hexene	2,4-dimethylhexane	others
SBA-16/Nb	90	2.5	0.0	11.6	0.0	83.1	0.0	5.3
		4	0.0	9.9	0.0	83.3	0.0	6.7
		6	0.0	11.1	0.0	82.8	0.0	6.1

	110	**2.5**	0.0	7.8	0.0	92.2	0.0	0.0
		4	0.0	6.0	0.0	94.0	0.0	0.0
		6	0.0	12.0	0.0	71.3	0.0	16.7
	130	**2.5**	0.0	11.5	0.0	78.9	0.0	9.6
		4	0.0	10.3	0.0	83.7	0.0	6.0
		6	0.0	8.2	0.0	81.6	0.0	10.2

As follows from Figure 5, the sample of SBA-16 impregnated with niobium is little active in HDO of phenol. The maximum phenol conversion was 6% for the process run at 130°C and hydrogen pressure of 6 MPa. At such a small conversion, besides the chemical compounds obtained as a result of phenol addition (denoted as other), two products were observed: 1-methoxycyclohexene (maximum selectivity of 12%) and 1-methoxy-2-hexene (maximum selectivity of 94%) which was the main product. No formation of cyclohexene, cyclohexanol or 2,4-dimethylhexane was detected. On the basis of the products of HDO reaction of phenol it can be inferred that the second pathway of transformations was realized. The increase in temperature and hydrogen pressure had no (or a little) effect on the process.

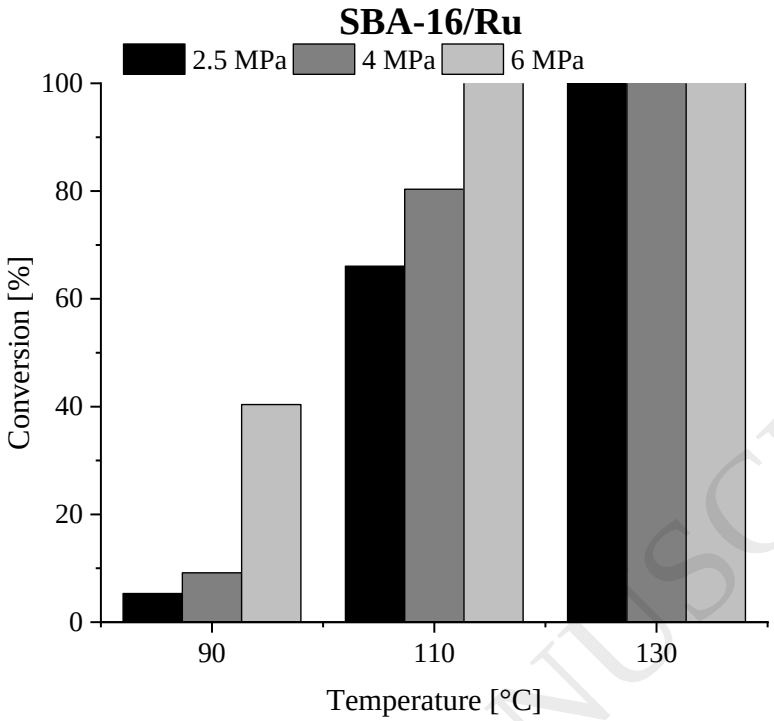

Figure 6. Conversion of phenol over SBA-16/Ru catalyst.

Table 4. Product distribution for phenol HDO over SBA-16/Ru catalyst under different conditions.

Catalyst	Temperature [°C]	Pressure [MPa]	Selectivity [%]					
			cyclohexene	1-methoxycyclohexene	cyclohexanol	1-methoxy-2-hexene	2,4-dimethylhexane	others
SBA-16/Ru	90	2.5	2.3	9.5	22.7	26.1	37.5	1.9
		4	1.1	16.6	32.0	6.7	43.6	0.0
		6	0.6	1.9	10.4	24.9	62.2	0.00

	110	**2.5**	1.0	0.7	38.3	3.4	56.4	0.2
		4	0.9	0.7	22.9	2.6	72.8	0.1
		6	0.9	0.4	3.8	0.2	94.7	0.0
	130	**2.5**	2.5	0.3	3.2	0.0	93.9	0.1
		4	1.4	0.7	3.9	2.6	90.9	0.5
		6	1.5	0.2	3.9	0.4	93.9	0.1

When the HDO of phenol is catalyzed by SBA-16/Ru, at all temperatures and pressures applied, the main reaction product was 2,4-dimethylhexane. With increasing temperature and hydrogen pressure, the conversion of phenol increased (Fig. 6). Full phenol conversion was obtained for the reaction performed at 110°C and hydrogen pressure of 6 MPa and adversary all reactions carried out at 130°C.When the reaction was performed at 90°C, besides the main product of 2,4-dimethylhexane relatively large amounts of cyclohexanol (maximum selectivity 32%)and 1-methoxy-2-hexene (maximum selectivity 26.1%) were formed. At a temperature by 20°C higher, the catalyst was selective towards the main product and cyclohexanol (maximum selectivity 38.3%).At 130°C, the formation of 2,4-dimethylhexane was observed with almost 94% selectivity.

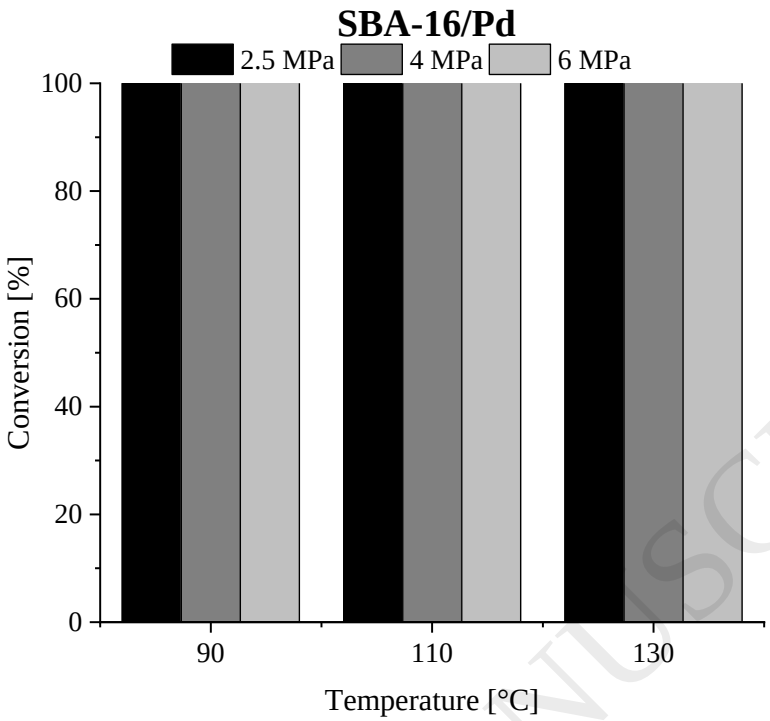

Figure 7. Conversion of phenol over SBA-16/Pd catalyst.

Table 5. Product distribution for phenol HDO over SBA-16/Pd catalyst under different conditions.

Catalyst	Temperature [°C]	Pressure [MPa]	Selectivity [%]					
			cyclohexene	1-methoxycyclohexene	cyclohexanol	1-methoxy-2-hexene	2,4-dimethylhexane	others
SBA-16/Pd	90	2.5	0.2	1.4	4.1	33.7	51.3	9.3
		4	0.8	0.5	2.9	0.0	73.8	22.0
		6	0.5	0.5	2.4	0.1	76.6	19.9

	110	**2.5**	1.0	1.0	4.4	0.0	67.0	26.6
		4	1.2	0.2	2.8	0.0	75.1	20.7
		6	1.0	0.9	3.9	0.2	72.5	21.5
	130	**2.5**	1.5	0.5	2.7	2.6	81.8	10.9
		4	1.6	0.5	3.2	2.8	68.2	23.7
		6	1.9	0.5	2.9	1.3	83.7	9.7

The palladium catalyst was even more active in HDO of phenol than the ruthenium one, as illustrated in Fig. 7. The main reaction product was 2,4-dimethylhexane, similarly as in the presence of SBA-16/Ru. Over the palladium catalyst in all temperature and hydrogen pressure variants 100% of phenol conversion was obtained. No significant influence of temperature and hydrogen pressure on the course of the process was noted. The catalytic system applied led to formation of phenol addition products (labelled as “other”) in the amounts reaching almost 27% at the expense of smaller amounts of 2,4-dimethylhexane.

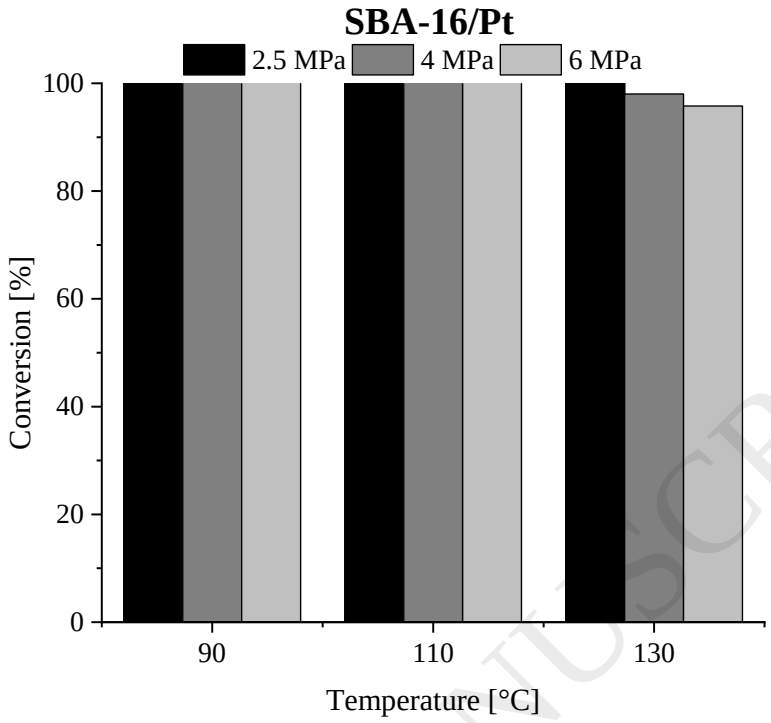

Figure 8. Conversion of phenol over SBA-16/Pt catalyst.

Table 6. Product distribution for phenol HDO over SBA-16/Pt catalyst under different conditions.

Catalyst	Temperature [°C]	Pressure [MPa]	Selectivity [%]					
			cyclohexene	1-methoxycyclohexene	cyclohexanol	1-methoxy-2-hexene	2,4-dimethylhexane	Others
SBA-16/Pt	90	2.5	17.4	1.3	4.7	0.0	76.6	0.0
		4	20.9	0.8	3.2	0.0	75.1	0.0
		6	20.4	0.8	4.1	0.0	74.6	0.1

	110	**2.5**	17.3	0.8	3.7	0.0	77.4	0.8
		4	19.9	0.6	3.6	0.1	75.6	0.2
		6	19.3	0.7	3.2	0.0	76.6	0.2
	130	**2.5**	17.3	0.2	3.8	0.1	78.4	0.2
		4	12.7	1.0	5.2	0.1	80.7	0.3
		6	10.2	0.4	5.0	0.2	84.2	0.0

Fig. 6 presents the results of the reaction catalyzed by SBA-16/Pt. The main product was also 2,4-dimethylhexane. In the presence of this catalyst some considerable amounts of cyclohexene were formed, for the reaction at 90°C and at hydrogen pressure of 4 MPa, the selectivity to cyclohexene was 21%. Thanks to the use of platinum as the active phase of the catalyst, a high degree of phenol deoxygenation and hydrogenation was achieved. In almost all temperature and pressure variants 100% phenol conversion was obtained. Similarly as in the presence of palladium catalyst, no effect of temperature and hydrogen pressure on the course of the process was noted.

To summarize, all the catalysts were active in the HDO of phenol and the most active catalysts were those containing Pd and Pt. It is worthy to stress that for those catalysts methyl group transfer and C-C bond cleavage were predominant. Contrary to that are numerous investigations, where HDO of phenol undergoes two main parallel routes with products presented in Table 7. The first route is direct deoxygenation (DDO) that leads to formation of benzene by the cleavage of C-O bond. The second is hydrogenation in which the aromatic ring is hydrogenated to cyclohexanol. Subsequent hydrogenation of benzene or deoxygenation of

cyclohexanol follows, leading to the formation of cyclohexane. In our case the main reaction product was an aliphatic hydrocarbon (not an aromatic hydrocarbon) and higher phenol conversion rates were obtained under milder temperature and pressure conditions.

Table 7. Reaction conditions, phenol conversion and product distribution for phenol HDO over different catalysts (literature data)

Catalyst	Temperature [°C]	H_2 pressure [MPa]	Main product	Selectivity [%]	Conversion [%]	Lit.
SiO_2/Pd	300	0.1	cyclohexanone	91.6	15.8	[35]
Nb_2O_5/Pd			benzene	80.2	6.6	
Al_2O_3/Pd	300	0.1	cyclohexanone	84.1	7.5	[36]
MCM-41/Pd	280	1	cyclohexane	63.0	80.0	[37]
Mo_2C/TiO_2	350	2.5	benzene	90.0	65.0	[38]
Ni/HZSM-5	200	5	cyclohexanone	44.0	9.0	[39]

Conclusions

The results of our experiment comprising the synthesis, physicochemical characterization and catalytic application of ordered mesoporous silica as supports of transition metals, permit drawing the following conclusions.

1. All synthesized materials are characterized by good textural and structural parameters, which has been established on the basis of XRD, TEM and low-temperature N_2sorption measurements, SEM/EDX, XPS measurements, TG analysis and H_2-TPR.

2. All synthesized materials are active in hydrodeoxygenation of phenol.
3. The type of metal on the surface of the silica support has direct impact on the degree of phenol conversion, type and amount of the reaction products. The activity of the catalysts obtained in HDO of phenol increases in the following order SBA-16/Nb < SBA-16/Ru < SBA-16/Pd < SBA-16/Pt.
4. The main product of the reaction, irrespectively of the reaction conditions was the branched hydrocarbon 2,4-dimethylhexane, characterized by the H/C ratio greater than that of phenol and with no oxygen in its structure.
5. The values of temperatures and pressures applied had impact on the degree of phenol conversion only when the reaction was performed over the catalyst SBA-16/Ru.
6. The values of temperatures and pressures applied had impact on the type and amounts of the reaction products in the presence of all catalysts applied.

Acknowledgments

National Science Centre is kindly acknowledged for the financial support (project no: DEC-2013/10/M/ST5/00652).

References

(1) Yujie, S.; Zhang, P.; Sua, Y. *Renew. Sust. Energ. Rev.*, **2015**, 50, 991.

(2) Zhong, W.; An, H.; Shen, L.; Fang, W.; Gao, X.; Dong, D. *Energ. Policy***2017**, 100, 365.

(3) McKendry, P. *Bioresource Technol.***2002**, 83, 37.

(4) He, Z.; Wang, X. *Catal. Sust. Energ.* **2012**, 1, 28.

(5) Vassilev, S. V.; Vassileva, C. G.; Vassilev, V. S. *Fuel*, **2015**, 158, 330.

(6) Liao, Y.; Liu, Q.; Wang, T.; Long, J.; Ma, L.; Zhang, Q. *Green Chem.***2014**, 16, 3305.

(7) Mohan, D.; Pittman, C. U.; Steele, P. H. *Energ. Fuel* **2006**, 20, 848.

(8) Mu, W.; Ben, H.; Du, X.; Zhang, X.; Hu, F.; Liu, W.; Ragauskas, A. J.; Deng, Y. *Bioresource Technol.***2014**, 173, 6.

(9) Kan, T.; Strezov, V.; Evans, T. J. *Renew. Sust. Energ. Rev.***2016**, 57, 1126.

(10) Sharifzadeh, M.; Richard, C.J.; Liu, K.; Hellgardt, K.; Chadwick, D.; Shah, N. *Biomass Bioenerg*. **2015**, 76, 108.

(11) Sharifzadeh, M.; Richard, C. J.; Liu, K.; Hellgardt, K.; Chadwick, D.; Shah, N. *Biomass Bioenerg.***2015**, 76, 108.

(12) Li, X.; Chen, G.; Liu, C.; Ma, W.; Yan, B.; Zhang, J. *Renew. Sust. Energ. Rev.***2017**, 71, 296.

(13) Bu, Q.; Lei, H.; Zacher, A. H.; Wang, L.; Ren, S.; Liang, J.; Wei, Y., Liu, Y.; Tang, J.; Zhang, Q.; Ruan, R. *Bioresource Technol.* **2012**, 124, 470.

(14) Shafaghat, H.; Rezaei, P. S.ü; Wan Daud, W. M. A. *J. Ind. Eng. Chem.* **2016**, 35, 268.

(15) De, S.; Saha, B.; Luque, R. *Bioresource Technol.***2015**, 178, 108.

(16) Arun, N.; Sharma, R. V.; Dalai, A. K. *Renew. Sust. Energ. Rev.***2015**, 48, 240.

(17) Liu, Y.; Chen, L.; Wang, T.; Zhang, Q.; Wang, C.; Yan, J.; Ma, L. *ACS Sustain. Chem. Eng.***2015**, 3, 1745.

(18) Byun, J.; Han, J. *Bioresource Technol*., **2016**, 211, 360.

(19) Jin, S.; Xiao, Z.; Li, C.; Chen, X.; Wang, L.; Xing, J.; Li, W.; Liang, C. *Catal. Today* **2014**, 234, 125.

(20) Patel, M.; Kumar, A.*Renew. Sust. Energ. Rev.*, **2016**, 58, 1293.

(21) Yao, G.; Wu, G.; Dai, W.; Guan, N.; Li, L. *Fuel*, **2015**, 150, 175.

(22) Güvenatam, B.; Kurşun, O.; Heeres, E. H. J.; Pidko, E. A.; Hensen, E. J. M. *Catal. Today***2014**, 233, 83.

(23) Lup, A. N. K.; Abnisa, F.; Daud, W. M. A. W.; Aroua, M. K. *J. Ind. Eng. Chem.***2017**, 56, 1.

(24) Li, X.; Luo, X.; Jin, Y.; Li, J.; Zhang, H.; Zhang, A.; Xie, J. *Renew. Sust. Energ. Rev.***2018**, 82, 3762.

(25) Nava, R.; Pawelec, B.; Castaño, P.; Alvarez- Galván, M. C.; Loricera, C. V.; Fierro, J. L. G. *Appl. Catal. B-Environ.***2009**, 92, 154.

(26) Kumar, P.; Guliants, V. V. *Micropor. Mesopor. Mat.***2010**, 132, 1.

(27) Bhanja, P.; Bhaumik, A. *Fuel***2016**, 185, 432.

(28) Ghampson, I.T.; Sepúlveda, C.; Garcia, R.; Fierro, J. L. G.; Escalona, N.; DeSisto, W. J. *Appl. Catal. A-Gen.* **2012**, 51, 435.

(29) Nowak, I.; Jaroniec, M. *Stud. Surf. Sci. Catal.***2007**, 165, 69.

(30) Grudzien, R.M.; Grabicka, B.E.; Jaroniec, M. *Appl. Surf. Sci.***2007**, 253, 5660.

(31) Hoffmann, F.; Cornelius, M.; Morell, J.; Fröba, M. *Angew. Chem. Int. Edit.***2006**, 45, 3216.

(32) Thommes, M.; Kaneko, K.; Neimark, A. V.; Olivier, J. P.; Rodriguez-Reinoso, F.; Rouquerol, J.; Sing, K. S. W. *Pure. Appl. Chem.***2015**, 87, 1051.

(33) Zhang, J.; Fidalgo, B.; Kolios, A.; Shen, D.; Gu, S. *Sust. Energy Fuels.* **2017**, 1, 1788.

(34) Sanna, A.; Vispute, T.P.; Huber, G.W. *Appl. Catal. B-Environ.* **2015**, *165*, 446.

(35) Barrios, A. M.; Teles, C. A.; Souza, P. M.; Rabelo-Neto, R. C.; Jacobs, G.; Davis, B. H.; Borges, L. E. P.; Noronha, F. B. *Catal. Today***2018**, 302, 115.

(36) Souza, P.M.; Rabelo-Neto, R.C.; Borges, L.E.P.; Jacobs, G.; Davis, B.H.; Graham, U.M.; Resasco, D.E.; Noronha, F.B. *ACS Catal.***2015**, 5, 7385.

(37) Zeng, Y.; Wang, Z.; Lin, W.; Song, W.; Christensen, J.M.; Jensen, A.D. *Catal. Commun.***2016**, 82, 46.

(38) Boullosa-Eiras, S.; Lodeng, R.; Bergem, H.; Stöcker, M.; Hannevold, L.; Blekkan, E.A. *Catal. Today*, **2014**, 223, 44.

(39) Zhao, C.; Kasakov, S.; He, J.; Lercher, J.A. *J. Catal*.**2012**, 296, 12.